Article

Cell Reports

Antisense RNA Controls LRP1 Sense Transcript Expression through Interaction with a Chromatin-Associated Protein, HMGB2

Graphical Abstract

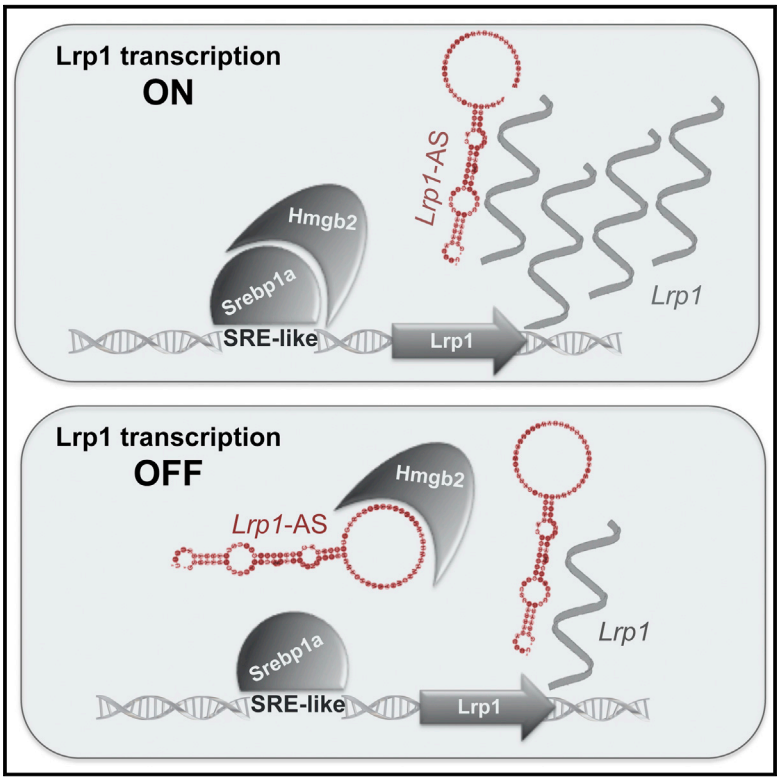

Highlights

- *LRP1*-AS is a conserved antisense ncRNA transcribed from the LRP1 locus
- The *Lrp1*-AS directly binds to Hmgb2
- Lrp1-AS inhibits Hmgb2-mediated Srebp1a transcriptional activation of *Lrp1*
- *LRP1*-AS expression is elevated in the brain of Alzheimer's disease patients

Authors

Yasunari Yamanaka, Mohammad Ali Faghihi, ..., Martin Lotz, Claes Wahlestedt

Correspondence

cwahlestedt@med.miami.edu

In Brief

Antisense noncoding RNAs are rapidly emerging as locus-specific regulators of gene expression in mammalian cells. Yamanaka et al. show that the antisense noncoding RNA *Lrp1*-AS negatively regulates Lrp1 expression by binding to Hmgb2 and inhibiting Hmgb2-mediated Srebp1a transcriptional activation of *Lrp1*. Moreover, they show discordant dysregulation of *LRP1*-AS and LRP1 expression in the brain of Alzheimer's disease patients.

Yamanaka et al., 2015, Cell Reports *11*, 967–976
May 12, 2015
http://dx.doi.org/10.1016/j.celrep.2015.04.011

Cell Reports
Article

Antisense RNA Controls LRP1 Sense Transcript Expression through Interaction with a Chromatin-Associated Protein, HMGB2

Yasunari Yamanaka,[1,3] Mohammad Ali Faghihi,[1] Marco Magistri,[1] Oscar Alvarez-Garcia,[2] Martin Lotz,[2] and Claes Wahlestedt[1,*]
[1]Center for Therapeutic Innovation and Department of Psychiatry and Behavioral Sciences, University of Miami Miller School of Medicine, Miami, FL 33136, USA
[2]Department of Molecular and Experimental Medicine, The Scripps Research Institute, La Jolla, CA 92037, USA
[3]Present address: RIKEN Research Cluster for Innovation, Wako, Saitama 351-0198, Japan
*Correspondence: cwahlestedt@med.miami.edu
http://dx.doi.org/10.1016/j.celrep.2015.04.011

SUMMARY

Long non-coding RNAs (lncRNAs), including natural antisense transcripts (NATs), are expressed more extensively than previously anticipated and have widespread roles in regulating gene expression. Nevertheless, the molecular mechanisms of action of the majority of NATs remain largely unknown. Here, we identify a NAT of low-density lipoprotein receptor-related protein 1 (*Lrp1*), referred to as *Lrp1*-AS, that negatively regulates *Lrp1* expression. We show that *Lrp1*-AS directly binds to high-mobility group box 2 (Hmgb2) and inhibits the activity of Hmgb2 to enhance Srebp1a-dependent transcription of *Lrp1*. Short oligonucleotides targeting *Lrp1*-AS inhibit the interaction of antisense transcript and Hmgb2 protein and increase *Lrp1* expression by enhancing Hmgb2 activity. Quantitative RT-PCR analysis of brain tissue samples from Alzheimer's disease patients and aged-matched controls revealed upregulation of LRP1-AS and downregulation of LRP1. Our data suggest a regulatory mechanism whereby a NAT interacts with a ubiquitous chromatin-associated protein to modulate its activity in a locus-specific fashion.

INTRODUCTION

Mammalian genomes are more extensively transcribed than expected, giving rise to thousands of long non-coding RNAs (lncRNAs), which are defined as RNA transcripts non-coding for protein and longer than 200 nt (Bertone et al., 2004; Birney et al., 2007; Carninci et al., 2005; Cheng et al., 2005; Djebali et al., 2012; Kapranov et al., 2007; Yelin et al., 2003). Among lncRNAs, NATs have emerged as a large class of regulatory long ncRNAs (Faghihi and Wahlestedt, 2009; Magistri et al., 2012). NATs are reported for more than 70% of all transcriptional units (Katayama et al., 2005) and 20% of human genes (Cheng et al., 2005; Yelin et al., 2003). We and others have recently shown that functional knockdown of NATs has positive or negative influences on the expression of neighboring protein-coding genes (Carrieri et al., 2012; Faghihi et al., 2008; Katayama et al., 2005; Mahmoudi et al., 2009; Modarresi et al., 2012), thus implying a critical role of NATs in the regulation of gene expression.

LncRNAs are implicated in numerous cellular processes ranging from pluripotency, differentiation, and cell-cycle regulation and are often dysregulated in disease states, such as Alzheimer's disease (AD), coronary artery disease, and cancer (Bond et al., 2009; Faghihi et al., 2008; Guttman et al., 2011; Harismendy et al., 2011; Hung et al., 2011; Pastori and Wahlestedt, 2012; Prensner et al., 2011; Velmeshev et al., 2013). Although the mechanisms of lncRNAs as key regulators of gene expression are yet to be fully elucidated, a common emerging theme is that lncRNAs form RNA-protein complexes to exert their regulatory functions. In some cases, NATs are reported to modulate DNA accessibility by binding to chromatin-modifying complexes and sequestration of transcription factor, which in turn influence gene expression (Guttman and Rinn, 2012; Pastori et al., 2010; Rinn and Chang, 2012; Wang and Chang, 2011). Therefore, in order to understand the function of lncRNAs, it is of crucial importance to identify the interacting proteins.

Low-density lipoprotein receptor-related protein (LRP) 1 is a member of the low-density lipoprotein receptor family, which has a role in a variety of physiological processes, including the cellular transport of cholesterol, endocytosis of ligands, and transcytosis across the blood-brain barrier (Lillis et al., 2008). Recently, LRP1 has been implicated in the systemic clearance of AD amyloid-beta (Aβ), and the level of LRP1 expression is critical for AD progression (Deane et al., 2008; Holtzman et al., 2012; Kang et al., 2000; Liu et al., 2007; Shibata et al., 2000). However, little is known about the mechanisms of *LRP1* expression regulation. Here, we showed that transcription of *LRP1* locus gives rise to both *LRP1* mRNA and a spliced NAT of *LRP1* gene, which we named *LRP1*-AS. We demonstrated that *LRP1*-AS negatively regulates *LRP1* gene expression through modulating the activity of the non-histone chromatin modifier HMGB2, and we showed

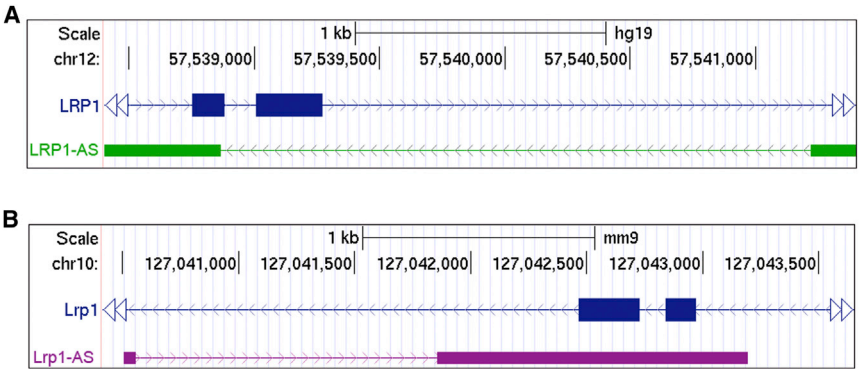

Figure 1. Genomic Organization of the Human LRP1 and Mouse *Lrp1* Locus

(A and B) NATs, human LRP1-AS (A) and mouse Lrp1-AS (B), are *cis* transcribed from the opposite strand of human LRP1 gene on chromosome 12 and mouse Lrp1 gene on chromosome 10, respectively. Exons 5 and 6 of LRP1 and Lrp1 are depicted in blue boxes; the exons of LRP1-AS and Lrp1-AS are depicted in green and violet boxes, respectively.

that *LRP1*-AS is elevated in the brains of AD patients, where it might repress LRP1 expression.

RESULTS

Identification of Human and Mouse *LRP1*-AS

To identify putative ncRNAs associated with human and mouse *LRP1* gene, we utilized the UCSC Genome Browser to search for Expressed Sequence Tags (ESTs) overlapping human and mouse LRP1 gene and checked for annotated antisense RNAs in Ensembl and AceView databases. We found ESTs from the opposite DNA strand of exon 5 of the human *LRP1* gene and exons 5 and 6 of the mouse *Lrp1* gene. In humans, these ESTs correspond to an Ensembl annotated two-exon antisense RNA of 645 bp (RP11-545N8.3) that we named LRP1-AS (Figure 1A). Similarly, in mouse, these ESTs correspond to an AceView (Thierry-Mieg and Thierry-Mieg, 2006) annotated two-exon antisense RNA of 1387 bp (sloty) that we named Lrp1-AS (Figure 1B). We found short open reading frames (ORFs) of 141 bp (15 to 155) and 108 bp (226 to 333) in exon 2 of human *LRP1*-AS. We also found short ORFs of 120 bp (388 to 507) and 117 bp (675 to 791) in exon 2 of mouse *Lrp1*-AS. The potential polypeptides had no sequence similarity to any other polypeptide sequence in the GenBank protein database and were not conserved with any predicted polypeptide in the Protein Clusters Database or the Conserved Domain Database. Exon 2 of *Lrp1*-AS directly overlaps the exons 5 and 6 of *Lrp1* by 395 bp, while exon 2 of *LRP1*-AS directly overlaps the exon 5 of *LRP1* by 119 bp (Figure S1A). This similar location of *LRP1*/*LRP1*-AS and *Lrp1*/*Lrp1*-AS has been maintained throughout evolution, indicating that this genomic arrangement might have a biological function. In order to derive general correlation between the reciprocal expression of LRP1 and LRP1-AS, we analyzed data from the Developmental Transcriptome project of the BrainSpan atlas (http://brainspan.org/) (Miller et al., 2014). This project consists of RNaseq data profiling up to 16 cortical and subcortical regions across the course of human brain development (13 developmental stages). The analysis of these data revealed a positive correlation between LRP1 and LRP1-AS expression across human brain development (Pearson $r = 0.6115$; $p < 0.0001$) (Figure S1B) and a reads per kilobase per million (RPKM) value for LRP1-AS that varies from 1 to 5.9. Depending of the total amount of RNA present in a single cell, it has been calculated that one copy of a transcript per cell corresponds to RPKM value between 0.5 and 5 (Mortazavi et al., 2008). Thus, in the human brain, there is approximately one transcript of LRP1-AS per cell. We then used digital PCR (dPCR) to measure the expression *of* Lrp1 and Lrp1-AS in the mouse brain and in variety of murine cells available in the lab. We noticed a general positive correlation between *Lrp1*-AS and *Lrp1* expression, with *Lrp1*-AS expressed at a higher level in the macrophage cell line RAW264.7 and at a lower level in pancreatic beta cell line MIN6 (Figure S2). Because of the higher expression in RAW264.7, we decided to utilize this cell line as a model to study the mechanism of function of Lrp1-AS.

Lrp1-AS Negatively Regulates *Lrp1* Expression

To investigate a possible regulation of *Lrp1* levels by *Lrp1*-AS, we analyzed changes in *Lrp1* levels after silencing *Lrp1*-AS expression. Silencing of *Lrp1*-AS by two different siRNAs targeting non-overlap regions in exons 2 led to a significant decrease in *Lrp1*-AS levels in RAW264.7 cells. We observed that the degree of *Lrp1-AS* downregulation was proportional to *Lrp1* mRNA and protein upregulation (Figures 2A and 2B). To confirm that knockdown of *Lrp1*-AS does not induce non-specific upregulation of other genes, we analyzed changes in *Gapdh* levels and found no change. We further examined *Lrp1* levels after overexpression of *Lrp1*-AS and observed a significant decrease in *Lrp1 expression* (Figure 2C). These data indicated that *Lrp1*-AS negatively regulates *Lrp1* expression, directly or indirectly, at both RNA and protein levels.

Cellular stress such as nutrient deprivation is known to influence the expression of Lrp1 (Annabi et al., 2010). In our cells after serum starvation, we observed upregulation of *Lrp*-AS and downregulation of *Lrp1* (Figure 2D). Together, these data showed that changes in *Lrp1*-AS levels influence *Lrp1* expression, and this regulation may be triggered by nutrient deprivation.

Identification of Hmgb2 Binding to *Lrp1*-AS

To identify specific proteins associated with *Lrp1*-AS RNA, we performed RNA chromatography on purified, in vitro-transcribed, full-length *Lrp1*-AS RNA, and 1.7-kb *Luc* mRNA as a negative control to probe nuclear extracts of RAW264.7 cells. Isolated proteins were run on a gel and visualized with silver staining; one differentially visible protein band was subjected to mass spectrometry, resulting in the identification of Hmgb2 (Figure S3). Consistently, the specificity of Hmgb2 binding to *Lrp1*-AS was confirmed by western blotting (WB) with specific

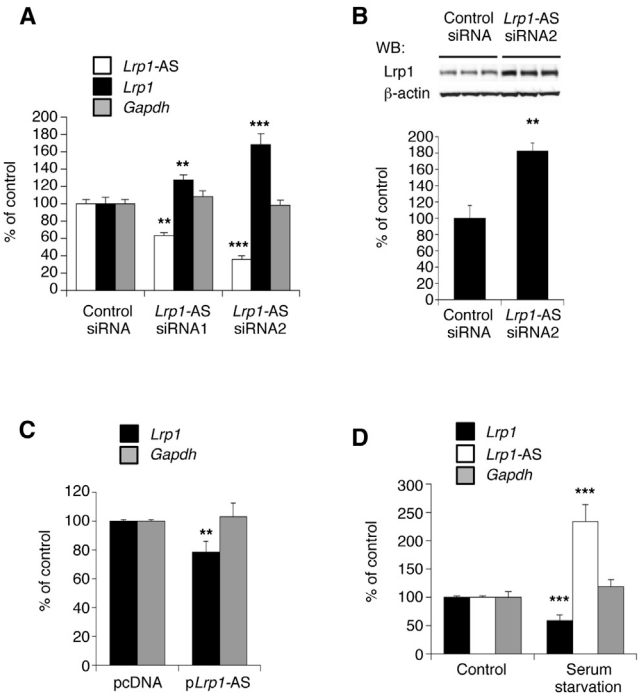

Figure 2. *Lrp1*-AS Negatively Regulates *Lrp1* Levels

(A) *Lrp1*, *Lrp1*-AS, *and Gapdh* RNA levels after *Lrp1*-AS silencing by control or two different siRNAs against *Lrp1*-AS in RAW264.7 cells. RNA levels were measured by quantitative RT-PCR of 24-hr post-transfection. Control siRNA has a sequence with no homology to any gene.

(B) WB analysis of Lrp1 and β-actin proteins in RAW264.7 cells treated with siRNA2 against Lrp1-AS (upper). Lrp1 protein levels were densitometrically quantified and normalized by β-actin (lower).

(C) *Lrp1* and *Gapdh* RNA levels after overexpression of *Lrp1*-AS in RAW264.7 cells. Empty vector (pcDNA) serves as a negative control.

(D) *Lrp1*-AS, *Lrp1*, and *Gapdh* RNA levels of RAW264.7 cells after 12-hr serum starvation.

Mean ± SD (n = 3 replicates) are shown in all bar graphs in (A) to (D). $^{**}p < 0.01$, $^{***}p < 0.001$ determined by ANOVA.

antibody (Figure 3A). Hmgb1/2 are the most abundant Hmg proteins regulating numerous cellular activities, including transcription, and Hmgb2 is highly expressed in lymphoid organs and testes (Ronfani et al., 2001). In the reciprocal experiment, we performed RNA immunoprecipitation (RIP) of endogenous Hmgb2 from RAW264.7 cells extracts. The anti-Hmgb2 IP retrieved associated *Lrp1*-AS RNA as detected by quantitative RT-PCR (qRT-PCR), but not nonspecific *Gapdh* or *β-actin* (Figure 3B).

Direct and Specific Binding of *Lrp1*-AS RNA to Hmgb2 Protein

Recently, Hmgb1/2 were shown to bind to a various immunogenic nucleic acids, including RNA (Yanai et al., 2009). To examine the direct interaction of Hmgb1/2 with nucleic acids, we purified recombinant Hmgb1/2 proteins from *E. coli* and subjected to in vitro binding assays with *Lrp1*-AS RNA. Hmgb1 and Hmgb2 were precipitated by immobilized full-length *Lrp1*-AS RNA, which was inhibited by free *Lrp1*-AS RNA in a dose-dependent manner (Figure 3C, left). Hmgb1-*Lrp1*-AS RNA binding was inhibited by genomic DNA, but Hmgb2-*Lrp1*-AS RNA binding was not affected (Figure 3C, right), suggesting the strong and specific binding of Hmgb2 to *Lrp1*-AS RNA. Moreover, we pulled down glutathione S-transferase (GST) fusion of Hmgb2 and found that *Lrp1*-AS RNA is associated with Hmgb2 protein (Figure 3D). Collectively, these experiments showed that *Lrp1*-AS RNA directly and specifically binds to Hmgb2.

We and others have previously shown that some lncRNAs, including NATs, can interact with sense transcripts and make RNA duplex through their overlap regions (Faghihi et al., 2008; Kretz et al., 2013). To test whether this is applied to *Lrp1*-AS, we performed in vivo RNase protection assay by qRT-PCR on *Lrp1* RNA. Single-stranded RNA was digested with RNase A, and *Lrp1* RNA fragment overlapped with *Lrp1*-AS was protected (Figure 3E), indicating that *Lrp1* and *Lrp1*-AS are capable of forming an RNA duplex at an overlapping region. To elucidate whether the overlap region of *Lrp1*-AS is functional, we performed RNA chromatography on two deletion mutants of *Lrp1*-AS, and we observed that the fragment (636–1,388) containing the overlap region with *Lrp1* strongly bound to Hmgb2 (Figures 3F and 3G). This result prompted us to investigate whether duplex of *Lrp1*-AS and *Lrp1* may modulate specific binding of *Lrp1*-AS to Hmgb2. Following RNA chromatography on *Lrp1* fragment and in vitro-hybridized RNA fragments duplex *Lrp1*-AS-*Lrp1* showed that *Lrp1* fragment does not bind to Hmgb2 (Figure 3H, lane 1) and that *Lrp1* inhibits *Lrp1*-AS fragment (636–1,388) from binding to Hmgb2 (Figure 3H, lanes 4 and 5). These data showed that Hmgb2 interacts with the overlap region of *Lrp1*-AS, but not *Lrp1*, and this interaction is inhibited by *Lrp1*.

Lrp1-AS Suppresses Hmgb2-Enhanced Activity of Srebp1a on *Lrp1* Transcription

Sterol regulatory element-binding proteins (SREBPs) are a family of three transcription factors that regulate expression of genes involved in lipid homeostasis and glucose metabolism (Jeon and Osborne, 2012; Raghow et al., 2008), and Srebp1/2 are known to interact with Hmgb1/2; their activity has been reported to be enhanced by Hmgb1 (Najima et al., 2005). Since Srebp2 was not expressed in RAW264.7 cells (data not shown), we focused on Srebp1a/c, which is also known to play a role in transcriptional regulation of *Lrp1* (Bown et al., 2011). To investigate a possible regulation of *Lrp1* by Hmgb1/2 via Srebp1a/c, we first analyzed changes in *Lrp1* levels after altering Srebp1 levels. Silencing of Srebp1 in RAW264.7 cells led to a significant decrease in *Lrp1* levels, but not *Lrp1*-AS (Figure 4A). Overexpression of Srebp1a-flag increased *Lrp1* levels (Figure 4B, lane 2), whereas Srebp1c-flag did not change *Lrp1* levels (Figure S4A). Together, these data showed that *Lrp1* is positively regulated by Srebp1a.

Next, to assess the effect of Hmgb1/2 on Srebp1 transcriptional activity, we examined *Lrp1* levels on overexpression of Hmgb1/2. Hmgb2, but not Hmgb1, increased Srebp1a-dependent *Lrp1* upregulation (Figure 4B, lanes 3 and 4). Srebp1a and Hmgb2 did not change *Lrp1*-AS levels (Figure S4B). Moreover, Hmgb2, but not Hmgb1, amplified Srebp1a-flag-induced *Lrp1* promoter activity (Figure 4C). To investigate the mechanisms for the functional cooperation between Srebp1a and Hmgb2, we examined their possible interactions. Reciprocal co-IP with

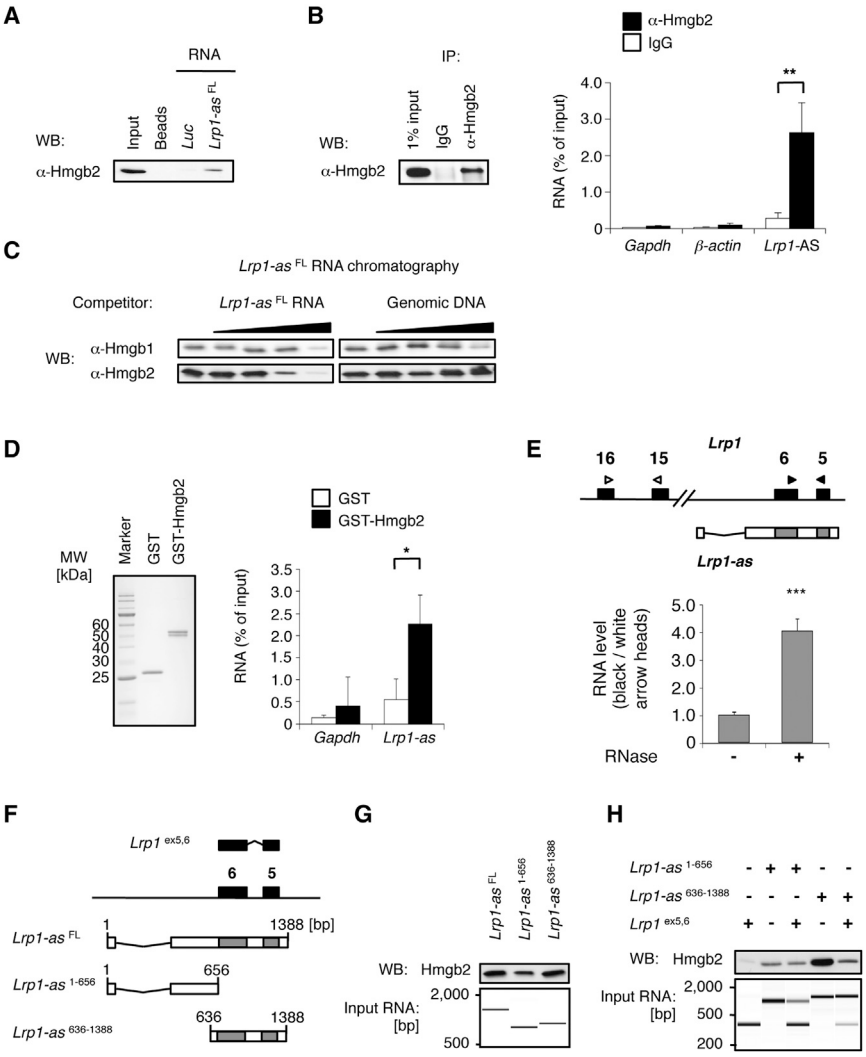

Figure 3. *Lrp1*-AS Binds to Hmgb2

(A) RNase-assisted RNA chromatography on full-length *Lrp1*-AS ^{FL} in RAW264.7 nuclear extracts, visualized by WB with specific antibody against Hmgb2.

(B) IP with control IgG or specific antibody against Hmgb2 from RAW264.7 lysates, visualized by WB (left), and co-precipitated RNAs from (B) were detected by qRT-PCR using primer pairs for *Lrp1*-AS, *Gapdh*, or *β-actin* (right).

(C) In vitro pull-down of 6XHis-tagged Hmgb2 with *Lrp1*-AS ^{FL} and free nucleic acids as indicated.

(D) In vitro pull-down of endogenous *Lrp1*-AS with GST or GST-fused Hmgb2 from RAW264.7 nuclear extracts. RNAs were detected by qRT-PCR using primer pairs for *Lrp1*-AS or *Gapdh* (right). Equal input proteins were visualized on electrophoresis by Comassie Brilliant Blue (CBB) stain (left). Mean ± SD (n = 3 replicates) are shown in all bar graphs. *p < 0.05, **p < 0.01 determined by ANOVA.

(E) RNase protection assay. The RNA ratios were calculated from qRT-PCR using primer pairs for overlap region (black arrowhead) or non-overlap region (white arrowhead) from RAW264.7 nuclear extracts treated with (+) or without (−) RNase A. Mean ± SD (n = 3 replicates) are shown. ***p < 0.001 determined by ANOVA.

(F) Schematic illustration of deletion constructs of *Lrp1* and *Lrp1*-AS used for (C) and (D): *Lrp1* construct contains exons 5 and 6 (395 bp) of *Lrp1*. *Lrp1*-AS $^{636–1388}$ construct contains the overlap region between *Lrp1* and *Lrp1*-AS, whereas *Lrp1*-AS $^{1–656}$ only contains the 5′ fragment of *Lrp1*-AS.

(G) RNA chromatography on full-length or fragments of *Lrp1*-AS, as indicated above, in RAW264.7 nuclear extracts, followed by WT (upper). Equal input RNAs were visualized on electrophoresis by Agilent Bioanalyzer (lower).

(H) RNA chromatography on *Lrp1*-AS fragments, *Lrp1* fragment, or *Lrp1*-AS:*Lrp1* fragments hybrid, as indicated above, in RAW264.7 nuclear extracts, followed by WB (upper). Equal input RNAs were visualized on electrophoresis by Agilent Bioanalyzer (lower).

specific antibodies and WB analyses demonstrated interaction of endogenous mature Srebp1 and Hmgb2 (Figures 4D and 4E). RNA chromatography on *Lrp1*-AS RNA failed to detect associated Srebp1, and IP of mature Srebp1 did not retrieve associated *Lrp1*-AS RNA (Figures S4A and S4B). These showed that Hmgb2 directly binds to Srebp1a in vivo and enhances its activity. Together, *Lrp1* upregulation by Srebp1a occurred at the level of transcription, and Hmgb2 directly enhances this regulation. We next examined whether *Lrp1*-AS could affect Hmgb2- and Srebp1a-dependent *Lrp1* transcriptional activation. Overexpression of *Lrp1*-AS repressed the potentiating effect of Hmgb2 on *Lrp1* upregulation by Srebp1a, but not Srebp1c (Figure 4F). *Lrp1*-AS decreased *Lrp1* promoter activity induced by Hmgb2 and Srebp1a (Figure 4G). Chromatin IP (ChIP) showed that *Lrp1*-AS depletion increased Srebp1 occupancy at two tandem SRE-like regions within *Lrp1* promoter (Figure 4H). To further investigate this regulatory mechanism, we measured Lrp1 expression in different tissues of Hmgb2 KO mice (Figure S5A). As expected, we observed a significant decrease in Lrp1 expression in the lungs of KO mice compared with WT. Unexpectedly, we observed an increase of Lrp1 expression in the spleen of KO animals and no significant changes in the brain, thymus, or testes. Srebp1 expression was significantly increased in the spleen of KO mice (Figure S5B), thus possibly explaining the increase of Lrp1 expression in this organ.

Collectively, these data showed that *Lrp1*-AS inhibits the ability of Hmgb2 to enhance Srebp1a-dependent transcription of *Lrp1*.

AntagoNAT Reveals a Functional Domain of *Lrp1*-AS Interacting with Hmgb2

We have previously shown that inhibition of NATs by oligonucleotide (termed as antagoNATs) induces upregulation of their sense transcripts and opens a new possibility that synthetically engineered DNAs could interact with both nucleic acids and protein functional domains to carry out engineered regulatory roles

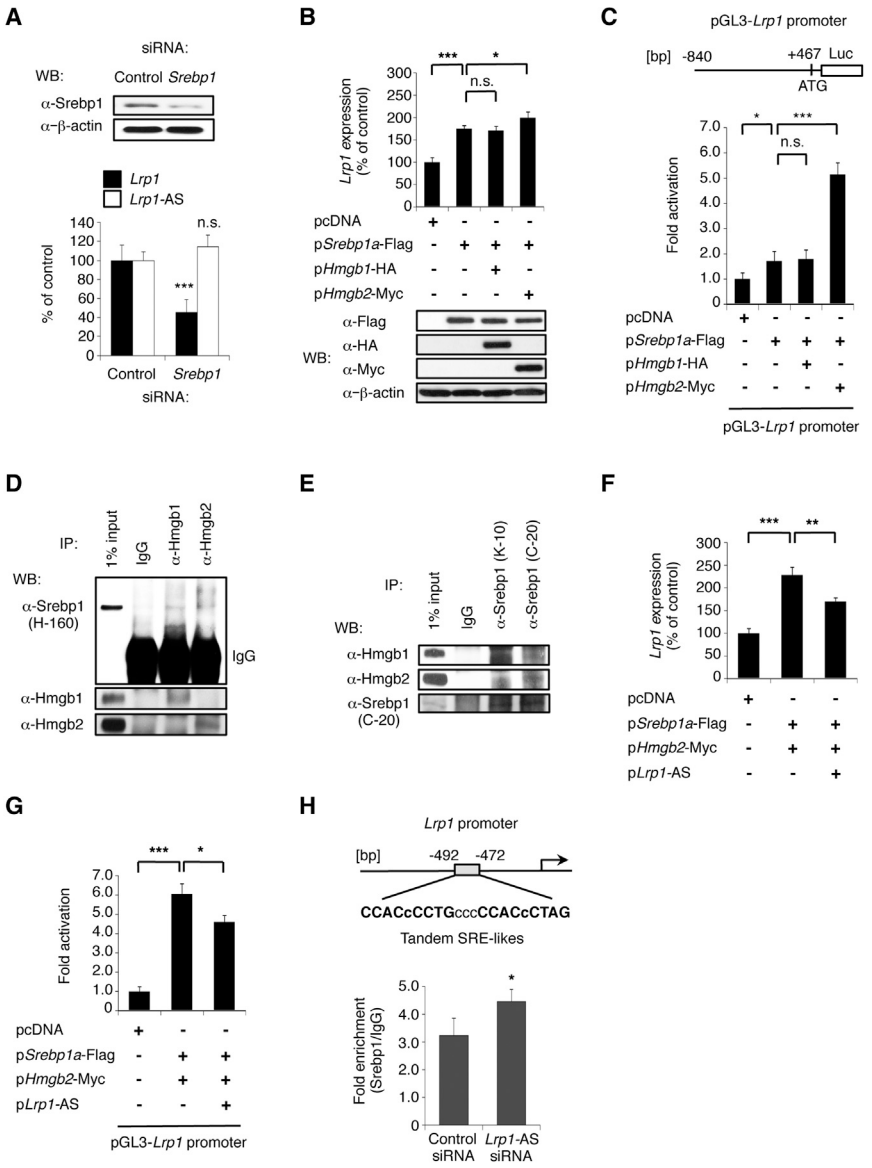

Figure 4. *Lrp1*-AS Reverses the Hmgb2-Mediated Increase in Srebp1-Dependent *Lrp1* Expression

(A) *Lrp1* and *Lrp1*-AS levels in RAW264.7 cells transfected with control or *Srebp1* siRNA. The control siRNA has a sequence with no homology to any gene. WB confirms Srebp1 silencing (upper).

(B) *Lrp1* levels after overexpression of mature Srebp1a-Flag and/or Hmgb1-HA/2-Myc in RAW264.7 cells (upper). Expression of exogenous proteins was monitored by WB with the indicated antibodies (lower). An antibody to β-actin was used as loading control in (A) and (B).

(C) Luciferase reporter assay after co-transfection of the *Lrp1* promoter-coupled luciferase construct (upper, pGK3-*Lrp1* pro.) together with overexpression of Srebp1-Flag and Hmgb1-HA/2-Myc in RAW264.7 cells. Firefly luciferase activity was normalized to *Renilla* luciferase activity.

(D and E) Reciprocal IP of endogenous Srebp1 or Hmgb1/2 from RAW264.7 cells followed by WB with the indicated antibodies. Rabbit IgG was used as negative control.

(F) *Lrp1* levels after overexpression of mature Srebp1a-Flag and Hmgb2-Myc with or without *Lrp1*-AS RNA in RAW264.7 cells.

(G) Luciferase activity after co-transfection of the *Lrp1* promoter-coupled luciferase construct together with overexpression of mature Srebp1-Flag and Hmgb2-Myc with or without *Lrp1*-AS RNA in RAW264.7 cells. Firefly luciferase activity was normalized to *Renilla* luciferase activity.

(H) Quantitative ChIP (qChIP) analysis with Srebp1 antibody or control IgG from RAW264.7 cells transfected with control or *Lrp1*-AS siRNA (lower). Diagram of the *Lrp1* promoter, showing the two tandem SREBP Responsive Elements-like motifs (SRE-likes in upper). Mean ± SD (n = 3 replicates) are shown in all bar graphs.*p < 0.05, **p < 0.01, ***p < 0.001 determined by ANOVA.

(Modarresi et al., 2012). We also observed that antagoNATs, which target the overlapping region between sense and antisense transcripts, produced the largest response in causing an increase in sense transcript expression (Modarresi et al., 2012).

To test whether antagoNATs could interfere the interactions of *Lrp1*-AS and, either Hmgb2 or *Lrp1*, we designed a series of 25 antagoNATs that target *Lrp1*-AS, covering ("walking") the entire shared sequence of *Lrp1*-AS and *Lrp-1* (Figure S6A). We observed that antagoNAT10 significantly increased *Lrp1* levels and simultaneously decreased *Lrp1*-AS levels (Figure 5A). We also used eight additional oligonucleotides, partially sharing sequence with antagoNAT10, to more exactly determine the potential domain of *Lrp1*-AS regulating *Lrp1* levels, and we observed similar effect with antagoNAT10e that was set shifting to 3′ by two bases from antagoNAT10 (Figures S6B and S6C). We further found that locked nucleic acid (LNA)-modified antagoNAT10 was more efficacious in increasing *Lrp1* levels (Figure S6D). We then performed in vivo RNase protection assay and found that antagoNAT10 failed to change the levels of preserved RNA (Figure 5B), indicating that the interaction between *Lrp1*-AS and *Lrp1* was not disrupted by antagoNAT10. This led us to test whether antagoNAT10 could modulate the binding of *Lrp1*-AS to Hmgb2. Co-transfection of AntagoNAT10 reversed the effect of *Lrp1*-AS on Hmgb2 and Srebp1-induced *Lrp1* levels (Figure 5C, lanes 4 and 5). The addition of AntagoNAT10, but not AntagoNAT control, efficiently inhibited *Lrp1*-AS retrieval by GST-Hmgb2 (Figure 5D). Together, these results suggests that antagoNAT against a part of the overlap region of *Lrp1*-AS inhibits the interaction between *Lrp1*-AS and Hmgb2, which is critical for regulating *Lrp1* levels (Figure 5E).

LRP1-AS Dysregulation in AD Brain

Previous reports have shown that *LRP1* levels are decreased in AD subjects, and the level of NAT is induced by diverse cell

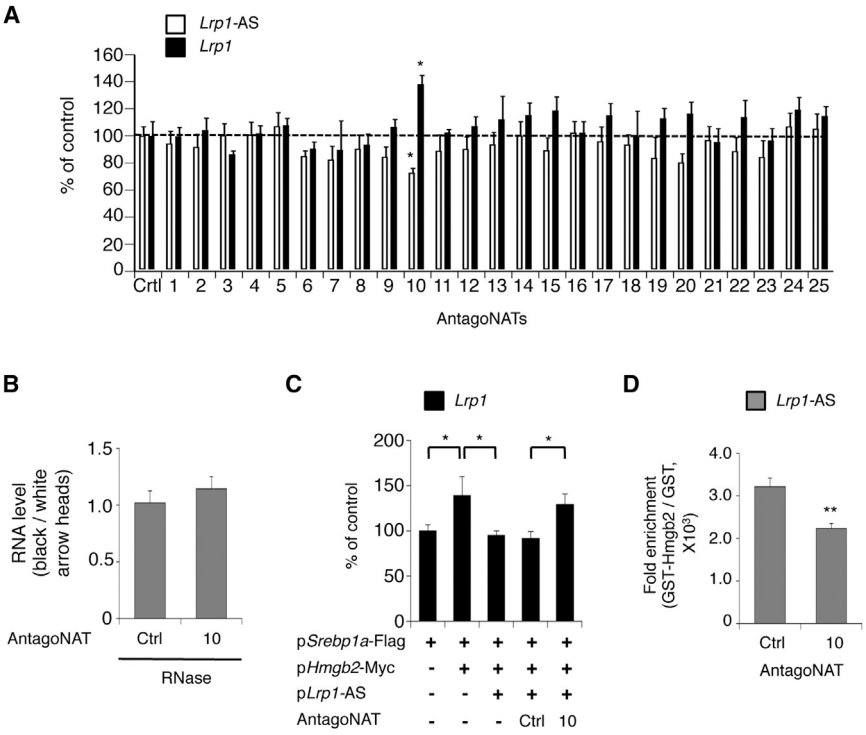

Figure 5. Blocking of *Lrp1*-AS-Hmgb2 Interaction by antagoNATs Induces *Lrp1* Expression

(A) *Lrp1* and *Lrp1*-AS levels of RAW264.7 cells transfected with control (Ctrl) or specific antagoNATs against *Lrp1*-AS, tiling the entire overlap region between *Lrp1* and *Lrp1*-AS (as in Figure S6). Control antagoNAT has a sequence with no homology to any gene.

(B) RNase protection assay. The RNA ratios were calculated from qRT-PCR using primer pairs for overlap region (black arrowhead) or non-overlap region (white arrowhead) as in Figure 3E from RAW264.7 nuclear extracts transfected with control (Ctrl) or antagoNAT10.

(C) *Lrp1* levels after overexpression of mature Srebp1a-Flag, Hmgb2-Myc, and *Lrp1*-AS RNA with control (Ctrl) or AntagoNAT10 in RAW264.7 cells.

(D) The in vitro translated *Lrp1*-AS was preincubated with control (Ctrl) or antagoNAT10 and pulled down with recombinant GST or GST-fused Hmgb2 as in Figure 3F. Associated *Lrp1*-AS RNAs were detected by qRT-PCR. Mean ± SD (n = 3 replicates) are shown in all bar graphs.*p < 0.05, **p < 0.01 determined by ANOVA.

stressors and elevated in AD subjects (Bishop et al., 2010; Faghihi et al., 2008; Saxena and Caroni, 2011). This prompted us to test whether *LRP1*-AS and LRP1 mRNA are dysregulated in the brain of AD patients. To test this hypothesis, we performed qRT-PCR using RNA extracted from the superior frontal gyrus of AD patients and age-matched controls to measure the expression of LRP1-AS and LRP1 mRNA. As previously reported, we observed decreased expression of LRP1 mRNA levels in AD subjects, while LRP1-AS levels were surprisingly increased (Figures 6A and 6B).

DISCUSSION

The multiple functions of lncRNAs are just starting to emerge, and the mechanisms through which they mediate their functions are subject to intense investigation. Here, we have identified a NAT, *Lrp1*-AS that has a critical role in the transcriptional regulation of *Lrp1* gene. The *Lrp1*-AS directly binds to Hmgb2 and inhibits Hmgb2-mediated Srebp1a transcriptional activity on *Lrp1*. Lrp1-AS function is in turn regulated by Lrp1 mRNA that can base pair with Lrp1-AS forming an RNA duplex, which prevents the interaction between Lrp1-AS and Hmgb2. Furthermore, antagoNAT against specific domain of *Lrp1*-AS inhibits the interaction between *Lrp1*-AS and Hmgb2, suggesting a model whereby a specific regulatory sequence of lncRNA is critical for its function.

In the nucleus, HMGBs are the most abundant regulatory proteins, which dynamically interact with chromatin and influence numerous activities, including transcription, replication, repair, and genomic stability (Bianchi and Agresti, 2005). HMGBs affect the chromatin fiber as architectural components by competing with histone H1 for chromatin binding sites and weakening its ability to restrict the access of transcription machinery to the chromatin (Bianchi and Agresti, 2005). These HMGBs-H1 interactions might facilitate nucleosome remodeling and regulate accessibility of transcription factors to the nucleosomal DNA in response to external stimuli. The NAT studied here interacts with HMGB2 and may serve as cell-type-specific natural RNA ligand to inhibit HMGB2 to exert their enhancer activities as a specific fine tuner. These suggest that a set of NATs interacts with ubiquitous regulatory proteins to form specific RNA-protein complexes that coordinate cell-type-specific gene expression patterns.

We and others provide evidence that HMGB functions as an RNA-binding proteins in addition to its long-recognized role as a DNA-binding protein (Yanai et al., 2009). HMGBs bind to chromatin without any known apparent preference for the underlying DNA sequence; their functional specificity could depend on direct interactions with sequence-specific transcriptional factors and bending of the DNA target sequences. However, many proteins that bind nucleic acids could be expected to display at least modest non-specific affinity for other nucleic acids, and even sequence-specific DNA-binding transcription factors appear to bind RNA with at least some sequence specificity. These examples include STAT1 transcription factor inhibited by an ncRNA in MHC expression, and TLS/FUS factor bound to RNA, which is involved in oncogenic chromosomal translocations (Lerga et al., 2001; Perrotti et al., 1998; Peyman, 1999). LncRNAs are *cis*- or *trans*-regulators, which can regulate target genes expression by acting as signals, guides, or scaffolds to the chromatin through interaction with chromatin proteins to change the epigenetic status of genes (Guttman and Rinn, 2012; Magistri et al., 2012; Rinn and Chang, 2012; Wang and Chang, 2011). In our

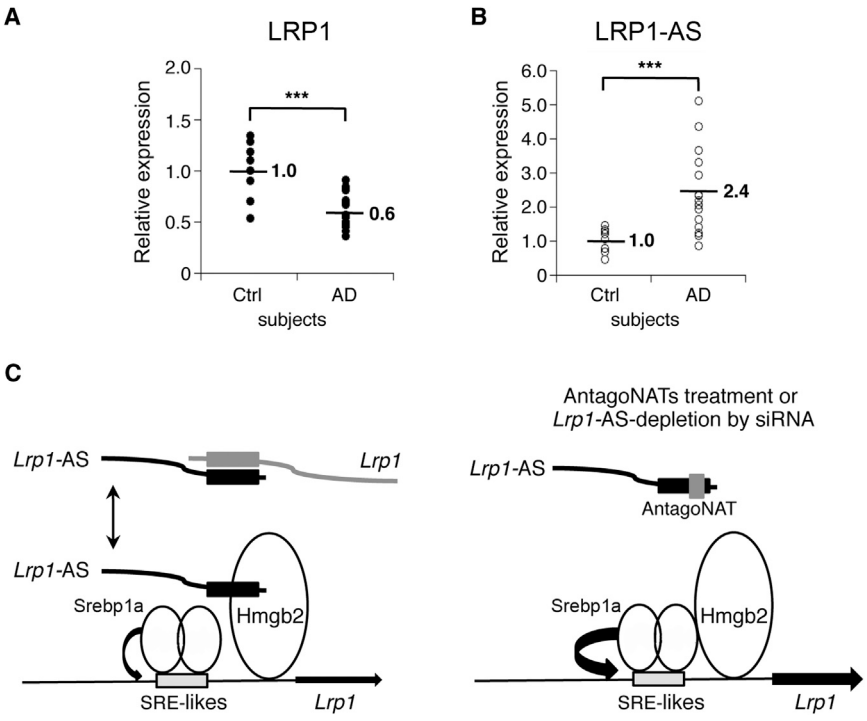

Figure 6. LRP1 and LRP1-AS Dysregulation in AD

(A and B) Quantitative RT-PCR analysis of LRP1 (A) and LRP1-AS (B) expression in superior frontal gyrus of 15 patients with AD and 8 control subjects (Ctrl). The housekeeping gene β-ACTIN was used as endogenous control; LRP1 and LRP1-AS expression was normalized to Ctrl. ***$p < 0.001$ determined by ANOVA.

(C) A model proposing functional and physical interactions between *Lrp1*-AS, Srebp1a, and Hmgb2 on the *Lrp1* Promoter. Hmgb2 can bind with Srebp1a and induces *Lrp1* promoter activity containing SRE-like motifs (depicted in gray boxes). When *Lrp1*-AS is depleted or treated with antagoNATs, cooperative activation of *Lrp1* expression by Hmgb2 and Srebp1a is enhanced.

studies, Lrp1-AS interacts with HMGB2 and may serve as cell-type- and locu-specific natural RNA ligand to fine tune HMGB2 activity. The specific sequence of the NAT resembles that of the protein's alternative target, and therefore, the NAT may compete for the protein binding to the target. This "molecular decoy" model was initially demonstrated in a study showing regulation of *E. coli* CsrA activity by a regulatory RNA called CsrB (Romeo, 1998). The regulatory RNAs can create new signaling pathways to regulate other transcriptional targets than those original targets. The degree of pairing of RNA-proteins may provide variations on global gene expression in cells, but exactly what regulatory mechanisms allow a NAT to bind to proteins should be elucidated. Complementary experiments may be needed to provide insight into the aspects of NAT sequence required for recognition by HMGB2, and this may make it clear whether there is specific sequence requirement in other NATs recognized by HMGB2. Finally, our study showed that LRP1 and LRP1-AS are discordantly dysregulated in the brain of AD patients compared with controls, where LRP1 is expressed at a lower level and LRP1-AS at a higher level. Further research is needed to investigate the functional implication of LRP1-AS in the pathological processes underlying AD, but accumulating findings suggest that NATs and other lncRNAs could potentially be pursued as diagnostic markers or therapeutic targets for different human diseases.

EXPERIMENTAL PROCEDURES

Cell Culture, Animal Studies, RNA Interference, Plasmids, and AntagoNATs

All animal experiments were performed according to protocols approved by the Institutional Animal Care and Use Committee at The Scripps Research Institute. RAW264.7 cell line (TIB-71, ATCC) was maintained in DMEM supplemented with 10% fetal bovine serum (Atlas Biologicals) and 1% Pen/Strep. *Lrp1*-AS siRNAs and control siRNA (AM4611) were synthesized by Ambion. Srebp-1 siRNA (sc-36558) was purchased from Santa Cruz Biotechnology. Mouse cDNAs were amplified by PCR (KOD Hot Start DNA Polymerase, Novagen). Full-length (1–1,388 bp), 5′ (1–656 bp), and 3′ (636–1,388 bp) *Lrp1*-AS and *Luciferase* gene (from pGL3 Basic Vector, Promega), 3XHA-tagged *Hmgb1*, and 3XMyc-tagged *Hmgb2* were cloned into pcDNA3.1 vector (Invitrogen). pcDNA3.1-Flag-tagged Srebp1a/c were kindly provided by Dr. Timothy Osborne (Sanford-Burnham Medical Research Institute). Cells were transfected with 30 nM of siRNA, 100 nM of antagoNATs, or 1 μg of plasmid using Amaxa 4D-Nucleofector (Lonza) according to manufacturer's instructions and harvested after 24- or 48-hr post-transfection. All oligonucleotide sequences are listed in Table S1.

RNA Purification and qRT-PCR Analysis

Total RNA from cells was isolated with RNeasy Plus Micro Kit (QIAGEN) as per manufacturer's instructions and analyzed with 2100 Bioanalyzer (Agilent). Reverse Transcription was performed using SuperScript III (Invitrogen) and random priming. Real-time PCR was performed with TaqMan Gene Expression Assays and HT7900 sequence detection system (Applied Biosystems), as previously described (Faghihi et al., 2008; Modarresi et al., 2012). Eukaryotic 18S or mouse β-actin was measured for an internal control and used for normalization. Details of the human brain samples were previously described (Faghihi et al., 2008). For RNA protection assays, cells were lysed in standard radioimmunoprecipitation assay (RIPA) buffer, incubated with or without RNase A/T1 (Ambion) for 1 hr at 37°C and then treated with proteinase K (Invitrogen) for 30 min at 37°C, followed by RNA extraction, as previously described (Faghihi et al., 2008).

GST Pull-Down Assays

GST-tagged Hmgb1/2 were expressed in BL21 *Escherichia coli* (Novagen) and purified according to standard protocols. Each GST-fusion protein was bound to glutathione beads (GE Healthcare) for 1chr at room temperature and then incubated with cell lysates for 2 hr at 4°C. After five washes with PBS, bound RNAs were extracted and analyzed by qRT-PCR. For in vitro binding assay, full-length *Lrp1*-AS was transcribed in vitro using MEGAscript T7 Kit (Ambion), treated with DNase I, purified with NucAway spin columns (Ambion), and denatured and refolded in RNA structure buffer (Ambion). The folded RNA was incubated with antagoNATs and GST-fusion protein for 1chr, and the complex was captured with glutathione beads for 1chr. After five times washes with PBS, bound RNA was extracted and analyzed by qRT-PCR.

RNase-Assisted RNA Chromatography

Full-length or fragment in vitro-transcribed 1.38 kb *Lrp1*-AS RNA or 1.8 kb fragment of *Luciferase* RNA was conjugated to adipic acid dehydrazide agarose beads (Sigma-Aldrich) as described. Briefly, the complexed beads were incubated with cell lysates for 2 hr at 37°C. After five washes, bound proteins were eluted with RNase A/T1 and V1 (Ambion) and visualized by Silver Staining Kit (GE Healthcare) or detected by WB. Selected band was subjected to mass spectrometry at The Scripps Research Institute. For RNA pull-down assays, 100 pmol of in vitro-transcribed *Lrp1*-AS RNAs were conjugated to beads and incubated with 10 pmol of recombinant 6XHis-tagged Hmgb1/2 (Prospec) in the presence of increasing amounts of free *Lrp1*-AS RNA (10, 100, 300, 1,000 pmol) or genomic DNA (50, 500, 1,500, 5,000 ng) for 2 hr at 37°C. After five washes, bound proteins were extracted and subjected to WB.

WB and IP

To prepare protein lysates, cells were harvested, washed, and lysed in standard RIPA buffer. Total protein concentration was measured by Pierce 660 nm protein assay, and WB was performed according to standard protocols. The quantification of signals was performed using Image J software. For IP, cells were cross-linked with 1% formaldehyde for 10 min, followed by the addition of glycine to a final concentration of 0.125 M. After two washes with PBS, cells were lysed with Buffer A (10 mM HEPES [pH 7.4], 10 mM KCl, 1.5 mM $MgCl_2$, 0.5 mM DTT supplemented with Roche Complete Protease Inhibitor Cocktail), lysed in 0.25% NP40, fractionated by low-speed centrifugation. The nuclear pellet was resuspended with Buffer C (20 mM HEPES [pH 7.4], 420 mM KCl, 4 mM $MgCl_2$, 0.5 mM DTT, 10% glycerol; Roche protease inhibitor) and sonicated for 7 min with Bioruptor UCD-200 (Diagenode). Combined nuclear and cytoplasmic fractions were mixed with antibody and incubated for 2 hr at 4°C. The complex was captured with Protein A/G beads for 1 hr at 4°C. After four times washes with NP-40 buffer (50 mM HEPES [pH 7.4], 100 mM KCl, 5 mM $MgCl_2$, 0.5 mM DTT, 0.1% NP-40, 10% glycerol), bound proteins were eluted in 2× Laemmli Sample Buffer and subjected to WB. For RIP, bound RNA were extracted with Proteinase K (Ambion) in RIPA buffer for 1 hr at 45°C and analyzed by qRT-PCR. Specific antibodies in the present study include Lrp1 (EPR3724, Novus Biologicals), Srebp-1 (H-160 for IP and ChIP, K-10 and C-20 for WB; Santa Cruz Biotechnology), Hmgb2 (H9789; Sigma-Aldrich), Flag (M2; Sigma-Aldrich), HA.11 (16B12; Covance), c-;*myc* (9E10; Covance), β-actin (AC-15; Sigma-Aldrich).

Luciferase Reporter Assays

pGL3-*Lrp1* promotor (Liu et al., 2007) was kindly provided by Dr. Guojun Bu (Mayo Clinic). Cell extracts after 24-hr transfection were assayed for firefly and renilla (phRL-TK; Promega) luciferase activities in 96-well white plates (Nunc) using Dual-luciferase Reporter Assay System (Promega) and EnVision 2104 Multilabel Reader (PerkinElmer).

ChIP

Cells were cross-linked with 1% formaldehyde for 10 min, followed by the addition of glycine to a final concentration of 0.125 M. After two washes with PBS, cells was lysed with Lysis Buffer 1 (50 mM HEPES [pH 7.4], 140 mM NaCl, 1 mM $MgCl_2$, 0.5% NP-40, 0.25% Triton X-100, 10% glycerol; Roche protease inhibitor) for 10 min, followed by Lysis Buffer 2 (10 mM Tris [pH 8.0], 200 mM NaCl, 1 mM EDTA, 0.5 mM EGTA; Roche protease inhibitor) for 10 min. Next, the nuclear pellet was sonicated for 40 min with Bioruptor UCD-200 in Lysis Buffer 3 (20 mM Tris [pH 8.0], 300 mM NaCl, 1 mM EDTA, 0.5 mM EGTA, 0.1% sodium deoxycholate, 0.5% N-Laurorylsarcosine, Roche protease inhibitor), and lysed in 1% Triton X-100. The nuclear fraction was mixed with antibody and incubated overnight at 4°C. The complex was captured with sheep anti-Rabbit IgG-coupled magnetic beads (Dynabeads; Invitrogen) for 1 hr at 4°C. After one wash with Low Salt Buffer (20 mM Tris [pH 8.0], 150 mM NaCl, 2 mM EDTA, 0.1% SDS, 1% Triton X-100), two washes with High Salt Buffer (20 mM Tris [pH 8.0], 400 mM NaCl, 2 mM EDTA, 0.1% SDS, 1% Triton X-100), five washes with RIPA Buffer and one time with TE Buffer (50 mM Tris [pH 8.0], 10 mM EDTA) containing 50 mM NaCl, bound DNA was reverse cross-linked in TE buffer with 1% SDS at 65°C overnight and treated with RNase A/T1 at 55°C for 30 min and following Proteinase K at 55°C for 1 hr. Bound DNA was purified and analyzed by qPCR with Power SYBR Green Master Mix (Applied Biosystems).

Raindance Raindrop dPCR Assay

dPCR assays were performed as per manufacturer's protocols. In brief, 50-μl reactions were used with Applied Biosystems 2X Taqman gene expression master mix, 20× primer probe, 25× drop stabilizer, and 100 ng of cDNA. Oil droplets were generated on the Raindrop Source chip instrument and then amplified on a BioRad C1000 thermocycler using the following conditions: 50°C for 2 min, 95°C for 10 min and 40 cycles of 95°C for 15 s, 60°C for 1 min, hold at 10°C. Fluorescent droplets were detected on the Raindance Raindrop Sense chip instrument and then analyzed using the Raindance Raindrop Analyst software v.2 to count VIC and FAM drops and to prepare output graphs.

SUPPLEMENTAL INFORMATION

Supplemental Information includes six figures and one table and can be found with this article online at http://dx.doi.org/10.1016/j.celrep.2015.04.011.

ACKNOWLEDGMENTS

This work was supported by U.S. NIH grants DA035592, MH084880, and NS071674 awarded to Claes Wahlested. NIH grant AG007996 was awarded to Martin Lotz. Yasunari Yamanaka was supported by the Japan Society for the Promotion of Science (21-8333). Some parts of this study were performed by the authors at The Scripps Research Institute in Florida.

Received: October 29, 2014
Revised: March 6, 2015
Accepted: April 3, 2015
Published: April 30, 2015

REFERENCES

Annabi, B., Doumit, J., Plouffe, K., Laflamme, C., Lord-Dufour, S., and Béliveau, R. (2010). Members of the low-density lipoprotein receptor-related proteins provide a differential molecular signature between parental and CD133+ DAOY medulloblastoma cells. Mol. Carcinog. *49*, 710–717.

Bertone, P., Stolc, V., Royce, T.E., Rozowsky, J.S., Urban, A.E., Zhu, X., Rinn, J.L., Tongprasit, W., Samanta, M., Weissman, S., et al. (2004). Global identification of human transcribed sequences with genome tiling arrays. Science *306*, 2242–2246.

Bianchi, M.E., and Agresti, A. (2005). HMG proteins: dynamic players in gene regulation and differentiation. Curr. Opin. Genet. Dev. *15*, 496–506.

Birney, E., Stamatoyannopoulos, J.A., Dutta, A., Guigó, R., Gingeras, T.R., Margulies, E.H., Weng, Z., Snyder, M., Dermitzakis, E.T., Thurman, R.E., et al.; ENCODE Project Consortium; NISC Comparative Sequencing Program; Baylor College of Medicine Human Genome Sequencing Center; Washington University Genome Sequencing Center; Broad Institute; Children's Hospital Oakland Research Institute (2007). Identification and analysis of functional elements in 1% of the human genome by the ENCODE pilot project. Nature *447*, 799–816.

Bishop, N.A., Lu, T., and Yankner, B.A. (2010). Neural mechanisms of ageing and cognitive decline. Nature *464*, 529–535.

Bond, A.M., Vangompel, M.J., Sametsky, E.A., Clark, M.F., Savage, J.C., Disterhoft, J.F., and Kohtz, J.D. (2009). Balanced gene regulation by an embryonic brain ncRNA is critical for adult hippocampal GABA circuitry. Nat. Neurosci. *12*, 1020–1027.

Bown, M.J., Jones, G.T., Harrison, S.C., Wright, B.J., Bumpstead, S., Baas, A.F., Gretarsdottir, S., Badger, S.A., Bradley, D.T., Burnand, K., et al.; CARDIoGRAM Consortium; Global BPgen Consortium; DIAGRAM Consortium; VRCNZ Consortium (2011). Abdominal aortic aneurysm is associated with a variant in low-density lipoprotein receptor-related protein 1. Am. J. Hum. Genet. *89*, 619–627.

Carninci, P., Kasukawa, T., Katayama, S., Gough, J., Frith, M.C., Maeda, N., Oyama, R., Ravasi, T., Lenhard, B., Wells, C., et al.; FANTOM Consortium; RIKEN Genome Exploration Research Group and Genome Science Group (Genome Network Project Core Group) (2005). The transcriptional landscape of the mammalian genome. Science *309*, 1559–1563.

Carrieri, C., Cimatti, L., Biagioli, M., Beugnet, A., Zucchelli, S., Fedele, S., Pesce, E., Ferrer, I., Collavin, L., Santoro, C., et al. (2012). Long non-coding antisense RNA controls Uchl1 translation through an embedded SINEB2 repeat. Nature *491*, 454–457.

Cheng, J., Kapranov, P., Drenkow, J., Dike, S., Brubaker, S., Patel, S., Long, J., Stern, D., Tammana, H., Helt, G., et al. (2005). Transcriptional maps of 10 human chromosomes at 5-nucleotide resolution. Science *308*, 1149–1154.

Deane, R., Sagare, A., Hamm, K., Parisi, M., Lane, S., Finn, M.B., Holtzman, D.M., and Zlokovic, B.V. (2008). apoE isoform-specific disruption of amyloid beta peptide clearance from mouse brain. J. Clin. Invest. *118*, 4002–4013.

Djebali, S., Davis, C.A., Merkel, A., Dobin, A., Lassmann, T., Mortazavi, A., Tanzer, A., Lagarde, J., Lin, W., Schlesinger, F., et al. (2012). Landscape of transcription in human cells. Nature *489*, 101–108.

Faghihi, M.A., and Wahlestedt, C. (2009). Regulatory roles of natural antisense transcripts. Nat. Rev. Mol. Cell Biol. *10*, 637–643.

Faghihi, M.A., Modarresi, F., Khalil, A.M., Wood, D.E., Sahagan, B.G., Morgan, T.E., Finch, C.E., St Laurent, G., 3rd, Kenny, P.J., and Wahlestedt, C. (2008). Expression of a noncoding RNA is elevated in Alzheimer's disease and drives rapid feed-forward regulation of beta-secretase. Nat. Med. *14*, 723–730.

Guttman, M., and Rinn, J.L. (2012). Modular regulatory principles of large non-coding RNAs. Nature *482*, 339–346.

Guttman, M., Donaghey, J., Carey, B.W., Garber, M., Grenier, J.K., Munson, G., Young, G., Lucas, A.B., Ach, R., Bruhn, L., et al. (2011). lincRNAs act in the circuitry controlling pluripotency and differentiation. Nature *477*, 295–300.

Harismendy, O., Notani, D., Song, X., Rahim, N.G., Tanasa, B., Heintzman, N., Ren, B., Fu, X.D., Topol, E.J., Rosenfeld, M.G., and Frazer, K.A. (2011). 9p21 DNA variants associated with coronary artery disease impair interferon-γ signalling response. Nature *470*, 264–268.

Holtzman, D.M., Herz, J., and Bu, G. (2012). Apolipoprotein E and apolipoprotein E receptors: normal biology and roles in Alzheimer disease. Cold Spring Harb Perspect Med *2*, a006312.

Hung, T., Wang, Y., Lin, M.F., Koegel, A.K., Kotake, Y., Grant, G.D., Horlings, H.M., Shah, N., Umbricht, C., Wang, P., et al. (2011). Extensive and coordinated transcription of noncoding RNAs within cell-cycle promoters. Nat. Genet. *43*, 621–629.

Jeon, T.I., and Osborne, T.F. (2012). SREBPs: metabolic integrators in physiology and metabolism. Trends Endocrinol. Metab. *23*, 65–72.

Kang, D.E., Pietrzik, C.U., Baum, L., Chevallier, N., Merriam, D.E., Kounnas, M.Z., Wagner, S.L., Troncoso, J.C., Kawas, C.H., Katzman, R., and Koo, E.H. (2000). Modulation of amyloid beta-protein clearance and Alzheimer's disease susceptibility by the LDL receptor-related protein pathway. J. Clin. Invest. *106*, 1159–1166.

Kapranov, P., Cheng, J., Dike, S., Nix, D.A., Duttagupta, R., Willingham, A.T., Stadler, P.F., Hertel, J., Hackermüller, J., Hofacker, I.L., et al. (2007). RNA maps reveal new RNA classes and a possible function for pervasive transcription. Science *316*, 1484–1488.

Katayama, S., Tomaru, Y., Kasukawa, T., Waki, K., Nakanishi, M., Nakamura, M., Nishida, H., Yap, C.C., Suzuki, M., Kawai, J., et al.; RIKEN Genome Exploration Research Group; Genome Science Group (Genome Network Project Core Group); FANTOM Consortium (2005). Antisense transcription in the mammalian transcriptome. Science *309*, 1564–1566.

Kretz, M., Siprashvili, Z., Chu, C., Webster, D.E., Zehnder, A., Qu, K., Lee, C.S., Flockhart, R.J., Groff, A.F., Chow, J., et al. (2013). Control of somatic tissue differentiation by the long non-coding RNA TINCR. Nature *493*, 231–235.

Lerga, A., Hallier, M., Delva, L., Orvain, C., Gallais, I., Marie, J., and Moreau-Gachelin, F. (2001). Identification of an RNA binding specificity for the potential splicing factor TLS. J. Biol. Chem. *276*, 6807–6816.

Lillis, A.P., Van Duyn, L.B., Murphy-Ullrich, J.E., and Strickland, D.K. (2008). LDL receptor-related protein 1: unique tissue-specific functions revealed by selective gene knockout studies. Physiol. Rev. *88*, 887–918.

Liu, Q., Zerbinatti, C.V., Zhang, J., Hoe, H.S., Wang, B., Cole, S.L., Herz, J., Muglia, L., and Bu, G. (2007). Amyloid precursor protein regulates brain apolipoprotein E and cholesterol metabolism through lipoprotein receptor LRP1. Neuron *56*, 66–78.

Magistri, M., Faghihi, M.A., St Laurent, G., 3rd, and Wahlestedt, C. (2012). Regulation of chromatin structure by long noncoding RNAs: focus on natural antisense transcripts. Trends Genet. *28*, 389–396.

Mahmoudi, S., Henriksson, S., Corcoran, M., Méndez-Vidal, C., Wiman, K.G., and Farnebo, M. (2009). Wrap53, a natural p53 antisense transcript required for p53 induction upon DNA damage. Mol. Cell *33*, 462–471.

Miller, J.A., Ding, S.L., Sunkin, S.M., Smith, K.A., Ng, L., Szafer, A., Ebbert, A., Riley, Z.L., Royall, J.J., Aiona, K., et al. (2014). Transcriptional landscape of the prenatal human brain. Nature *508*, 199–206.

Modarresi, F., Faghihi, M.A., Lopez-Toledano, M.A., Fatemi, R.P., Magistri, M., Brothers, S.P., van der Brug, M.P., and Wahlestedt, C. (2012). Inhibition of natural antisense transcripts in vivo results in gene-specific transcriptional upregulation. Nat. Biotechnol. *30*, 453–459.

Mortazavi, A., Williams, B.A., McCue, K., Schaeffer, L., and Wold, B. (2008). Mapping and quantifying mammalian transcriptomes by RNA-Seq. Nat. Methods *5*, 621–628.

Najima, Y., Yahagi, N., Takeuchi, Y., Matsuzaka, T., Sekiya, M., Nakagawa, Y., Amemiya-Kudo, M., Okazaki, H., Okazaki, S., Tamura, Y., et al. (2005). High mobility group protein-B1 interacts with sterol regulatory element-binding proteins to enhance their DNA binding. J. Biol. Chem. *280*, 27523–27532.

Pastori, C., and Wahlestedt, C. (2012). Involvement of long noncoding RNAs in diseases affecting the central nervous system. RNA Biol. *9*, 860–870.

Pastori, C., Magistri, M., Napoli, S., Carbone, G.M., and Catapano, C.V. (2010). Small RNA-directed transcriptional control: new insights into mechanisms and therapeutic applications. Cell Cycle *9*, 2353–2362.

Perrotti, D., Bonatti, S., Trotta, R., Martinez, R., Skorski, T., Salomoni, P., Grassilli, E., Lozzo, R.V., Cooper, D.R., and Calabretta, B. (1998). TLS/FUS, a pro-oncogene involved in multiple chromosomal translocations, is a novel regulator of BCR/ABL-mediated leukemogenesis. EMBO J. *17*, 4442–4455.

Peyman, J.A. (1999). Repression of major histocompatibility complex genes by a human trophoblast ribonucleic acid. Biol. Reprod. *60*, 23–31.

Prensner, J.R., Iyer, M.K., Balbin, O.A., Dhanasekaran, S.M., Cao, Q., Brenner, J.C., Laxman, B., Asangani, I.A., Grasso, C.S., Kominsky, H.D., et al. (2011). Transcriptome sequencing across a prostate cancer cohort identifies PCAT-1, an unannotated lincRNA implicated in disease progression. Nat. Biotechnol. *29*, 742–749.

Raghow, R., Yellaturu, C., Deng, X., Park, E.A., and Elam, M.B. (2008). SREBPs: the crossroads of physiological and pathological lipid homeostasis. Trends Endocrinol. Metab. *19*, 65–73.

Rinn, J.L., and Chang, H.Y. (2012). Genome regulation by long noncoding RNAs. Annu. Rev. Biochem. *81*, 145–166.

Romeo, T. (1998). Global regulation by the small RNA-binding protein CsrA and the non-coding RNA molecule CsrB. Mol. Microbiol. *29*, 1321–1330.

Ronfani, L., Ferraguti, M., Croci, L., Ovitt, C.E., Schöler, H.R., Consalez, G.G., and Bianchi, M.E. (2001). Reduced fertility and spermatogenesis defects in mice lacking chromosomal protein Hmgb2. Development *128*, 1265–1273.

Saxena, S., and Caroni, P. (2011). Selective neuronal vulnerability in neurodegenerative diseases: from stressor thresholds to degeneration. Neuron *71*, 35–48.

Shibata, M., Yamada, S., Kumar, S.R., Calero, M., Bading, J., Frangione, B., Holtzman, D.M., Miller, C.A., Strickland, D.K., Ghiso, J., and Zlokovic, B.V. (2000). Clearance of Alzheimer's amyloid-ss(1-40) peptide from brain by LDL receptor-related protein-1 at the blood-brain barrier. J. Clin. Invest. *106*, 1489–1499.

Thierry-Mieg, D., and Thierry-Mieg, J. (2006). AceView: a comprehensive cDNA-supported gene and transcripts annotation. Genome Biol *7* (*Suppl 1*), S12.1–14.

Velmeshev, D., Magistri, M., and Faghihi, M.A. (2013). Expression of non-protein-coding antisense RNAs in genomic regions related to autism spectrum disorders. Mol. Autism *4*, 32.

Wang, K.C., and Chang, H.Y. (2011). Molecular mechanisms of long noncoding RNAs. Mol. Cell *43*, 904–914.

Yanai, H., Ban, T., Wang, Z., Choi, M.K., Kawamura, T., Negishi, H., Nakasato, M., Lu, Y., Hangai, S., Koshiba, R., et al. (2009). HMGB proteins function as universal sentinels for nucleic-acid-mediated innate immune responses. Nature *462*, 99–103.

Yelin, R., Dahary, D., Sorek, R., Levanon, E.Y., Goldstein, O., Shoshan, A., Diber, A., Biton, S., Tamir, Y., Khosravi, R., et al. (2003). Widespread occurrence of antisense transcription in the human genome. Nat. Biotechnol. *21*, 379–386.